Preprints of the 19th World Congress
The International Federation of Automatic Control
Cape Town, South Africa. August 24-29, 2014

Observer-based controller design for networked predictive control of an automotive drivetrain with backlash

C. F. Caruntu and C. Lazar

Department of Automatic Control and Applied Informatics,
The "Gheorghe Asachi" Technical University of Iasi, Romania
(e-mail: {caruntuc,clazar}@ac.tuiasi.ro)

Abstract: State feedback control is very attractive due to the precise computation of the gain matrix, but the implementation of a real-state feedback controller is impossible in most of the practical situations. Hence the need for an estimator or observer is obvious to estimate all the state variables by observing the input and the output of the controlled system. As such, the purpose of the paper is to provide a control design strategy based on a Luenberger observer that can assure the closed-loop performances of a vehicle drivetrain with backlash, while compensating the network-induced time-varying delays. The designed robust full state-feedback predictive controller based on flexible control Lyapunov functions explicitly takes into account the time-varying delays and guarantees also the input-to-state stability of the system in a non-conservative way. The control strategy was experimentally tested on a vehicle drivetrain emulator controlled through Controller Area Network.

Keywords: Networked control systems, observer design, predictive control, automotive drivetrain.

1. INTRODUCTION

The advanced control techniques, which rely on full state feedback, rather than classic output feedback, became increasingly attractive for different control applications in the last years. However, the implementation of a real-state feedback controller is possible only when all state variables are directly measurable. This condition is almost impossible to accomplish due to the excess number of required sensors or unavailability of states for measurement in most of the practical situations. Hence the need for an estimator or observer is obvious to estimate the state variables by observing the input and the output of the controlled system. While observer design for linear discrete-time systems is a trivial problem, observer design for piecewise linear plant models raises considerable difficulties (Spinu et al., 2012). In the literature there are papers that address the design of observers for continuous-time switched affine systems (Alessandri and Coletta, 2001), bi-modal piecewise linear systems in both continuous and discrete time (Juloski et al., 2007), discrete-time systems with piecewise affine dynamics (Heemels et al., 2008), discrete-time systems with input-induced bilinearity (Spinu et al., 2012), disturbed networked control systems (Postoyan and Nesic, 2012) and nonlinear systems with delayed measurements (Ahmed-Ali et al., 2013).

Moreover, backlash introduces a hard nonlinearity in the control loop for torque generation and distribution, which is a common problem in powertrain control. This phenomenon occurs whenever there is a gap in the transmission link, resulting in an angular position difference between wheels and engine, which leads to zero torque transmitted through the shaft. The effect of traversing the backlash gap is a large shaft torque and sudden acceleration of the vehicle. Controlling of mechanical systems with backlash nonlinearities is a topic of increasing interest (Rostalski et al., 2007; Templin, 2008), because it can lead to reduced performances and even instability. Engine control systems must compensate for the backlash with the purpose of traversing it as fast as possible. New driveline management application and high-powered engines increase the need for strategies on how to apply the engine torque in an optimal way. Furthermore, the components of the control system are linked using a communication network, e.g., Controller Area Network (CAN), which brings up the challenge of dealing with the effects of the network-induced delays in the control loop because they can be time-varying, may degrade the performances and can even destabilize the networked control systems (NCSs) designed without considering them.

As such, the problem considered in this paper is the development of a networked predictive control strategy, based on the design of a Luenberger observer, which is applied to minimize the backlash effects in a vehicle drivetrain, while compensating the CAN-induced time-varying delays. The proposed solution starts by deriving a piecewise linear (PWL) model of a two inertias drivetrain, which takes into consideration the backlash nonlinearity and the effects of the network-induced time-varying delays by using a disturbance method. Then, a Luenberger observer which estimates all the states is synthesized for the discrete-time system with PWL dynamics. Afterwards, a robust one step ahead MPC scheme is designed using the concept of flexible control Lyapunov functions (CLF) that explicitly accounts for rejection of disturbances introduced by the time-varying delays and guarantees also the input-to-state stability of the system in a non-conservative way. The control strategy was implemented in Matlab/Simulink to control the physical plant (vehicle drivetrain) on a real-time simulation test-bench and the designed experiments validate the proposed approach.

Notation and basic definitions. $\mathbb{R}$, $\mathbb{R}_+$, $\mathbb{Z}$ and $\mathbb{Z}_+$ are the real, non-negative real, integer and non-negative integer numbers.

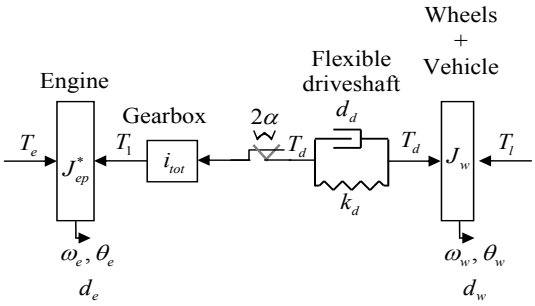

Fig. 1. Schematic representation of a vehicle drivetrain.

$\mathbb{R}^{n\times m}$ denotes the set of real $n \times m$ matrices. We use the notation $\mathbb{Z}_{\geq c_1}$ and $\mathbb{Z}_{(c_1,c_2]}$ to denote the sets $\{k \in \mathbb{Z}_+ \mid k \geq c_1\}$ and $\{k \in \mathbb{Z}_+ \mid c_1 < k \leq c_2\}$, respectively, for some $c_1, c_2 \in \mathbb{Z}_+$. Let $\|x\|_\infty := \max_{i\in\mathbb{Z}_{[1,n]}} |[x]_i|$, where $|\cdot|$ denotes the absolute value. A function $\varphi : \mathbb{R}_+ \to \mathbb{R}_+$ belongs to class $\mathcal{K}$ if it is continuous, strictly increasing and $\varphi(0) = 0$. A function $\varphi : \mathbb{R}_+ \to \mathbb{R}_+$ is said to belong to class $\mathcal{K}_\infty$ if it is of class $\mathcal{K}$ and $\lim_{s\to\infty} \varphi(s) = \infty$. A polyhedron (or a polyhedral set) in $\mathbb{R}^n$ is a set obtained as the intersection of a finite number of open and/or closed half-spaces. Let $\mathcal{P}(\mathbb{R}^n)$ denote the set of all bounded and non-empty polyhedrons in $\mathbb{R}^n$. Given a polyhedron $\mathbb{P} \in \mathcal{P}(\mathbb{R}^n)$, the map vert: $\mathcal{P}(\mathbb{R}^n) \rightrightarrows \mathbb{R}^n$ provides a set of vertices of cl($\mathbb{P}$).

2. DRIVETRAIN MODELING

Fig. 1 is a schematic representation of a vehicle drivetrain with backlash, having two inertias, one for the engine and gearbox (J^*_{ep}), and another one for the vehicle and the driving wheels (J_w) connected through a flexible driveshaft. The engine generates a torque (T_e), which is transmitted to the wheels through the driveline. Backlash nonlinearity exists in almost all gear boxes and in many mechanical couplings, being a common problem in vehicle drivetrains. The modeling of a mechanical system with backlash has to consider two different operational modes: backlash (non-contact) mode (when the two mechanical components are not in contact) and contact mode (when there is contact between the two mechanical components resulting in a moment transmission).

2.1 Mathematical description

The equations that describe the engine and wheel dynamics are:

$$\begin{aligned} J^*_{ep}\dot{\omega}_e &= T_e - F_{bck}\frac{T_d}{i_{tot}} - d_e\omega_e, \\ J_w\dot{\omega}_w &= F_{bck}T_d - d_w\omega_w - T_l \end{aligned} \tag{1}$$

where θ_e and θ_w are the engine and wheel angles, ω_e and ω_w are the engine and wheel angular velocities, $\dot{\omega}_e$ and $\dot{\omega}_w$ are the engine and wheel angular accelerations, respectively, i_{tot} is the overall gear ratio, d_e and d_w are the engine and wheel damping coefficients, T_l is the load torque and F_{bck} is the backlash force that equals 0 when the systems is in the backlash (non-contact) mode, and equals 1 if the system is in the contact mode.

The torque in the driveshaft is modeled as

$$T_d = k_d\left(\frac{\theta_e}{i_{tot}} - \theta_w\right) + d_d\left(\frac{\dot{\theta}_e}{i_{tot}} - \dot{\theta}_w\right), \tag{2}$$

where k_d and d_d represent the stiffness and damping coefficients of the flexible driveshaft.

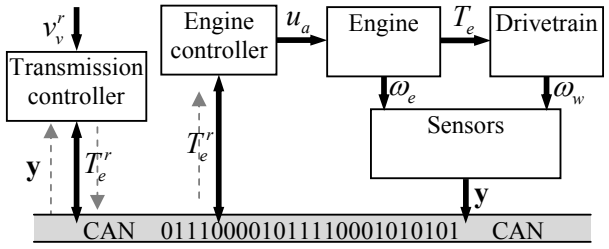

Fig. 2. Drivetrain control architecture.

Starting from equations (1), that describe the dynamics of the engine and wheel inertias, and considering, without loss of generality, that there is a fixed transmission ratio and no load torque, a state-space model of the system is obtained:

$$\begin{cases} \dot{x} = A_{ci}x + B_c u \text{ if } x \in \mathbb{P}_i \\ y = C_c x \end{cases}, \tag{3}$$

$$\begin{aligned} x &= \left[\begin{array}{cc} \omega_e & \omega_w & \frac{\theta_e}{i_{tot}} - \theta_w \end{array}\right]^T, \\ u &= [\,T_e\,] \end{aligned} \tag{4}$$

where $i \in \mathcal{I} := \mathbb{Z}_{[1,2]}$ denoting the active mode at time $t \in \mathbb{R}_+$. The collection of sets $\{\mathbb{P}_i | i \in \mathcal{I}\}$ defines a partition of the state-space $\mathbb{X} \subseteq \mathbb{R}^3$ as follows:

$$\begin{cases} \mathbb{P}_1 := \{x \in \mathbb{R}^3 | |x_3| \leq \alpha\} \\ \mathbb{P}_2 := \{x \in \mathbb{R}^3 | |x_3| > \alpha\} \end{cases} \tag{5}$$

where α is the backlash angle. The input of the system is represented by the engine torque, the system states are the engine and wheel angular velocities and the torsional angle between engine and wheels and the outputs are the first two states.

For the contact mode using $F_{bck} = 1$, the system matrices yield

$$\begin{aligned} A_{c1} &= \begin{bmatrix} -\frac{d_e+\frac{d_d}{i^2_{tot}}}{J^*_{ep}} & \frac{d_d}{i_{tot}J^*_{ep}} & -\frac{k_d}{i_{tot}J^*_{ep}} \\ \frac{d_d}{i_{tot}J_w} & -\frac{d_d+d_w}{J_w} & \frac{k_d}{J_w} \\ \frac{1}{i_{tot}} & -1 & 0 \end{bmatrix}, \\ B_c &= \begin{bmatrix} \frac{1}{J^*_{ep}} \\ 0 \\ 0 \end{bmatrix}, C_c = \begin{bmatrix} 1 & 0 & 0 \\ 0 & 1 & 0 \end{bmatrix}. \end{aligned} \tag{6}$$

In a similar way, the non-contact mode is characterized by transmitting no torque from the engine to the wheels ($F_{bck} = 0$), which yields the following system matrix

$$A_{c2} = \begin{bmatrix} -\frac{d_e}{J^*_{ep}} & 0 & 0 \\ 0 & -\frac{d_w}{J_w} & 0 \\ \frac{1}{i_{tot}} & -1 & 0 \end{bmatrix}, \tag{7}$$

and matrices B_c and C_c are the same as for the contact mode.

2.2 Network-controlled architecture

In Fig. 2 it can be seen that the components of the networked vehicle drivetrain control system, e.g., sensors, controller, actuator, communicate through a shared network.

The complete network-controlled architecture, which is graphically illustrated in Fig. 2, operates as follows:

- the outputs of the system are measured by sensors and samples are sent to the controller through CAN;
- the transmission controller receives the measurements from the sensors and the desired vehicle velocity reference

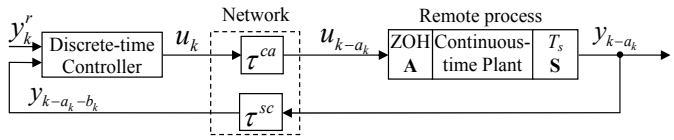

Fig. 3. NCS with time delays.

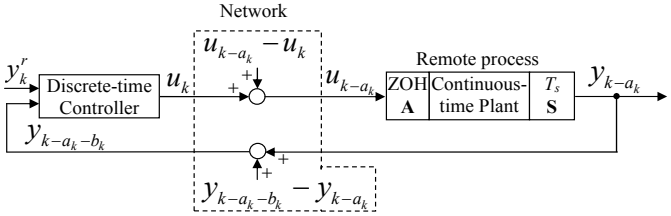

Fig. 4. NCS with time delays as disturbances.

$v_v^r = r_w\omega_w^r$ and calculates the required torque, while handling the physical constraints and the delays; r_w is the wheel radius and ω_w^r is the desired wheel speed;
- the control signal (the torque calculated by the controller) is sent to the engine controller through CAN;
- the engine controller actuates the spark timing and airflow (through u_a) as requested for driveline control.

The dashed lines depicted in Fig. 2 represent the direction of the messages. In what follows, a model of the drivetrain that accounts for backlash and the time-varying delays induced by CAN is developed, followed by the transmission controller design in Section 3.

2.3 Network delay modeled as disturbance

The standard NCS illustrated in Fig. 3 is composed of five parts: a shared communication network, a physical plant, a sensor node (S), a controller node and an actuator node (A). The network-induced delays, which can be smaller and larger than the sampling period, are denoted as τ^{ca} (the delay in the forward channel) and as τ^{sc} (the delay in the feedback channel). It can be observed that Fig. 3 is equivalent to Fig. 4, in which the difference between the actual control signal and the delayed one is regarded as a hypothetical disturbance (Natori et al., 2008). Furthermore, the difference between the actual output and the delayed one is regarded as another hypothetical disturbance (Caruntu and Lazar, 2011).

Notation: Let a_k and b_k denote the delay in the forward and feedback channels at time instant k, expressed as a number of sampling periods: $a_k = \lceil \tau_k^{ca}/T_s \rceil$, $b_k = \lceil \tau_k^{sc}/T_s \rceil$, where T_s is the sampling period of the system. Moreover, let $\bar{a}$ and $\bar{b}$ denote the maximum delays in the forward and feedback channels expressed as a number of sampling periods: $\bar{a} = \lceil \tau^{ca^{max}}/T_s \rceil$, $\bar{b} = \lceil \tau^{sc^{max}}/T_s \rceil$.

The physical plant is given by the discrete-time state-space model (Caruntu et al., 2011b)

$$\begin{cases} x_{k+1} = A_{di}x_k + B_{di}u_k + \sum_{j=0}^{a_k} \Delta_{j,k}(u_{k-j-1} - u_{k-j}), \\ y_k = C_d x_k \end{cases}, \tag{8}$$

where x_k is the system state, u_k is the control signal, $A_{di} = e^{A_{ci}T_s}$, $B_{di} = \int_0^{T_s} e^{A_{ci}(T_s-\theta)}d\theta B_{ci}$ and $C_d = C_c$ are the discrete-time system matrices and

$$\Delta_{j,k} = \begin{cases} 0, & \tau_{k-j}^{ca} - jT_s \le 0 \\ \int_0^{\tau_{k-j}^{ca} - jT_s} e^{A_{ci}(T_s-\theta)}d\theta B_{ci}, & 0 < \tau_{k-j}^{ca} - jT_s < T_s \\ \int_0^{T_s} e^{A_{ci}(T_s-\theta)}d\theta B_{ci}, & T_s \le \tau_{k-j}^{ca} - jT_s \end{cases} \tag{9}$$

for all $k \in \mathbb{Z}_+$ and $j \in \mathbb{Z}_{[0,a_k]}$ with

$$\tau_k^{ca} \ge \tau_{k-1}^{ca} - T_s. \tag{10}$$

Forward channel delays The maximum discrete-time forward channel disturbance representation is given by

$$u_k^d = u_{k-a_k} - u_k. \tag{11}$$

In (Caruntu and Lazar, 2012) it is shown that if the input of the plant is bounded then all possible disturbances that appear due to the forward channel time-varying delays can be included in a bounded set $\mathbb{W}_u$.

Considering that the control signal is lower and upper bounded

$$u^{min} \le u_k \le u^{max}, \tag{12}$$

where u^{min} and u^{max} are the minimum and the maximum control signal values, the disturbance can be bounded as (Caruntu and Lazar, 2012)

$$u^{min} - u^{max} \le u_k^d \le u^{max} - u^{min}. \tag{13}$$

Moreover, if the control signal is incrementally restricted

$$-u^{\Delta} \le \Delta u_k \le u^{\Delta}, \tag{14}$$

where $\Delta u_k := u_k - u_{k-1}$, for all $k \in \mathbb{Z}_{\ge 1}$, with u_0 some predetermined value and u^{Δ} the maximum increase/decrease of the control signal at each sampling time instant $k \in \mathbb{Z}_{\ge 1}$, the disturbance can be rebounded as (Caruntu and Lazar, 2012)

$$-\bar{a}u^{\Delta} \le u_k^d \le \bar{a}u^{\Delta}. \tag{15}$$

Feedback channel delays The hypothetical disturbance exerted on the physical plant gives the following discrete-time feedback channel disturbance representation

$$y_k^d = y_{k-a_k-b_k} - y_{k-a_k}. \tag{16}$$

In (Caruntu and Lazar, 2011) it is shown that if the input of the plant is bounded then all possible disturbances that appear due to the feddback channel time-varying delays can be inclued in a bounded set $\mathbb{W}_y$.

Consider the physical plant (8) with input disturbance

$$\begin{cases} x_{k+1} = A_{di}x_k + B_{di}(u_k + u_k^d) = \\ = A_{di}^l x_{k-l+1} + \sum_{j=0}^{l-1} A_{di}^j B_{di}(u_{k-j} + u_{k-j}^d), \\ y_k = C_d x_k \end{cases} \tag{17}$$

then, (16) becomes

$$\begin{aligned} y_k^d = C((I_n - A_{di}^{b_k})x_{k-a_k-b_k-1} - \\ - \sum_{j=0}^{b_k-1} A_{di}^j B_{di}(u_{k-a_k-j-2} + u_{k-a_k-j-2}^d)) \end{aligned} \tag{18}$$

Notice that, $x_{k-a_k-b_k}$ is known at time instant k, all u_{k-j}, $j \in \mathbb{Z}_{\ge 1}$ are known, all u_{k-j}^d, $j \in \mathbb{Z}_{\ge 1}$ are bounded, a_k and b_k are bounded by $\bar{a}$ and $\bar{b}$, respectively, so x_k^d can be dynamically bounded at each sampling instant $k \in \mathbb{Z}_+$.

Now, the output that reaches the controller becomes

$$y_k = Cx_k = C(A_{di}x_{k-1} + B_{di}u_{k-1}) + w_k, \tag{19}$$

where $w_k = C(B_{di}u_{k-1}^d) + y_k^d$.

The time-varying delays give a time-varying disturbance, but the sets $\mathbb{W}_u$, which is defined by $C(B_{di}u_{k-1}^d)$, and $\mathbb{W}_y$, which is defined by y_k^d, remain fixed. This modeling technique is suitable for the use of the results presented in (Lazar and Heemels, 2008), in which the disturbances are explicitly taken into account during the design phase of the predictive controller.

3. PREDICTIVE CONTROLLER WITH LUENBERGER OBSERVER DESIGN

3.1 Luenberger observer design

Assumption 3.1. The region of the discrete-time PWL vehicle drivetrain model $\mathbb{P}_i$, such that $\begin{bmatrix}\hat{x}\\ u\end{bmatrix} \in \mathbb{P}_i$, is known at each moment of time.

The Luenberger observer can be written as follows:

$$\begin{cases} \hat{x}_{k+1} = A_{di}\hat{x}_k + B_{di}u_k + L_i(y-\hat{y}), \\ \hat{y} = C_d\hat{x}. \end{cases} \tag{20}$$

From Assumption 3.1 it follows that for any $\begin{bmatrix}\hat{x}\\ u\end{bmatrix} \in \mathbb{P}_i$, $\begin{bmatrix}x\\ u\end{bmatrix} \in \mathbb{P}_i$ and as such, the error dynamics is

$$e_{k+1} = (A_{di} - L_iC_d)e_k. \tag{21}$$

Theorem 3.2. Suppose there exists a positive definite matrix P and a number $\rho \in \mathbb{R}_{(0,1)}$ and

$$(A_{di} - L_iC_d)^\top P(A_{di} - L_iC_d) \preceq \rho P, \tag{22}$$

hold for all $i \in \mathbb{Z}_{[1,s]}$. Then the error dynamics (21) is globally asymptotically stable.

To solve the inequality (22) in Theorem 3.2 the following lemma is introduced.

Lemma 3.3. Suppose that

$$\begin{bmatrix} \rho P & A_{di}^\top P - C_d^\top Y_i \\ PA_{di} - Y_i^\top C_d & P \end{bmatrix} \preceq 0 \tag{23}$$

holds for all $i \in \mathbb{Z}_{[1,s]}$ and some $P \succ 0, \rho \in \mathbb{R}_{(0,1)}$ and Y_i. Then the inequality (22) holds with P, ρ and $L_i = (Y_iP^{-1})^\top$.

For the proof of Theorem 3.2 and Lemma 3.3 the interested reader is referred to Theorem 1 and Lemma 1 from (Alessandri and Coletta, 2001). Note that it is possible to compute a single gain $L = L_i$ for the discrete-time PWL observer by considering a single $Y = Y_i$ in (23).

3.2 Robust one step ahead predictive controller design

The flexible Lyapunov function concept was proposed in (Lazar, 2009) by extending and relaxing the conventional Lyapunov condition. These functions offer a stability guarantee (under a recursive feasibility assumption) even for a short prediction horizon. In this paper, the concept was used in designing a robust one step ahead MPC scheme to attain stability and performance. Also, the disturbances are explicitly taken into account during the design phase by using input-to-state stability (ISS) concepts.

Consider the perturbed discrete-time constrained nonlinear drivetrain system (19) with the observer (20). Naturally, it is assumed that the set of feasible states $\mathbb{X}$, the set of feasible inputs $\mathbb{U}$ and the disturbance set $\mathbb{W}$ are bounded polyhedra with non-empty interiors containing the origin. Next, let $\alpha_1, \alpha_2, \alpha_3 \in \mathcal{K}_\infty$ and let $\sigma \in \mathcal{K}$.

Definition 3.4. A function $V : \mathbb{R}^n \to \mathbb{R}_+$ that satisfies

$$\alpha_1(\|\hat{x}\|) \le V(\hat{x}) \le \alpha_2(\|\hat{x}\|), \quad \forall \hat{x} \in \mathbb{X} \subseteq \mathbb{R}^n \tag{24}$$

and for which there exists a possibly set-valued control law $\pi : \mathbb{R}^n \rightrightarrows \mathbb{U}$ such that

$$\begin{aligned} V(A_{di}\hat{x}_k + B_{di}u_k + w_k + L_i(y-\hat{y})) - V(\hat{x}) \le \\ \le -\alpha_3(\|\hat{x}\|) + \sigma(\|w\|), \\ \forall \hat{x} \in \mathbb{X}, \forall u \in \pi(\hat{x}), \forall w \in \mathbb{W}, \end{aligned} \tag{25}$$

is called an *input-to-state stability control Lyapunov function (ISS-CLF)* in $\mathbb{X}$ for system (19) and disturbances in $\mathbb{W}$.

ISS theory (see (Jiang and Wang, 2001)) can be used to derive an input-to-state stabilizing predictive control scheme with improved disturbance rejection, as done in (Lazar and Heemels, 2008), where this property is refereed to as *optimized ISS*.

As such, let $\mathbb{W}$ be a convex hull of the vertices $w^e, e = 1, \dots, E$, and let λ_k^e, $k \in \mathbb{Z}_+$, be optimization variables associated with each vertex w^e. Let $J(\lambda^1, \dots, \lambda^E, \lambda) : \mathbb{R}_+^E \times \mathbb{R}_+ \to \mathbb{R}_+$ be a strictly convex, radially unbounded function (i.e. $J(\cdot)$ tends to infinity when its arguments tend to infinity) and let $J(\lambda^1, \dots, \lambda^E, \lambda) \to 0 \Rightarrow \lambda^e \to 0$ for all $e = 1, \dots, E$ and $\lambda \to 0$, and $J(0, \dots, 0, 0) = 0$.

Choose off-line a CLF $V(\cdot)$ for system (19) without disturbances and let $\alpha_3 \in \mathcal{K}_\infty$ and $\hat{x} \in \mathbb{X}$ be given. At each control sampling instant $k \in \mathbb{Z}_+$ the one step ahead ISS MPC controller solves the following problem.

Problem 3.5. At time $k \in \mathbb{Z}_+$ obtain the observed state $\hat{x}_k$ and minimize the cost $J(\lambda_k^1, \dots, \lambda_k^E, \lambda_k)$ over $u_k, \lambda_k^1, \dots, \lambda_k^E$ and λ_k, subject to the constraints

$$u_k \in \mathbb{U},\ (A_{di}\hat{x}_k + B_{di}u_k + L_i(y-\hat{y})) \in \mathbb{X},\ \lambda_k^e \ge 0, \lambda_k \ge 0, \tag{26a}$$

$$V(A_{di}\hat{x}_k + B_{di}u_k + L_i(y-\hat{y})) - V(\hat{x}_k) + \alpha_3(\|\hat{x}_k\|) \le \lambda_k, \tag{26b}$$

$$V(A_{di}\hat{x}_k + B_{di}u_k + L_i(y-\hat{y}) + w^e) - V(\hat{x}_k) + \alpha_3(\|\hat{x}_k\|) \le \lambda_k^e, \tag{26c}$$

for all $e = 1, \dots, E$. □

Let $\pi(\hat{x}_k) := \{u_k \in \mathbb{R}^m \mid \exists \lambda_k, \lambda_k^e, e \in \mathbb{Z}_{[1,E]} \text{ s.t. (26) holds}\}$ and let $\phi_{\text{cl}}(\hat{x}_k, \pi(\hat{x}_k), w_k) := \{A_{di}\hat{x}_k + B_{di}u_k + w_k + L_i(y - \hat{y}) \mid u_k \in \pi(\hat{x}_k)\}$ denote the difference inclusion corresponding to system (19) in closed-loop with the set of feasible solutions obtained by solving Problem 3.5 at each sampling instant $k \in \mathbb{Z}_+$.

Next, the main robust stability result in terms of ISS is stated. This result is an adaptation of the main result in (Lazar and Heemels, 2008), to fit the relaxation (26b) of Problem 3.5, i.e., $\lambda_k = 0$ for all $k \in \mathbb{Z}_+$ corresponds to the problem considered in (Lazar and Heemels, 2008).

Theorem 3.6. Let $\alpha_1, \alpha_2, \alpha_3 \in \mathcal{K}_\infty$, a continuous and convex CLF $V(\cdot)$ and a cost $J(\cdot)$ be given. Suppose that Problem 3.5 is feasible for all states x in $\mathbb{X}$ and assume that $\lim_{k\to\infty} \lambda_k^* = 0$. Then, the trajectories generated by the difference inclusion

$$\hat{x}_{k+1} \in \phi_{cl}(\hat{x}_k, \pi(\hat{x}_k), w_k), \quad k \in \mathbb{Z}_+, \tag{27}$$

with initial state $\hat{x}_0 = x_0 \in \mathbb{X}$ converge in finite time to a robustly positively invariant subset of $\mathbb{X}$, in which the difference inclusion is ISS for disturbances in $\mathbb{W}$.

The proof of Theorem 3.6 follows from standard arguments employed in proving ISS and Lyapunov stability and is therefore omitted here. The interested reader is referred to (Lazar and Heemels, 2008) and (Lazar, 2009) for more details. Advantageous properties of the proposed robust controller are that ISS is guaranteed for any (feasible) solution of the optimization problem, state and input constraints can be explicitly accounted for, and feedback to disturbances is provided actively, on-line. The key of the stability proof is the limiting condition $\lim_{k\to\infty} \lambda_k^* = 0$. In what follows a non-conservative solution for guaranteeing this condition is provided.

Lemma 3.7. Let $\Delta \in \mathbb{R}_+$ be a fixed constant to be chosen a priori and let $\rho \in \mathbb{R}_{[0,1)}$ and $M \in \mathbb{Z}_{>0}$. If

$$0 \leq \lambda_k \leq \rho^{\frac{1}{M}}(\lambda_{k-1}^* + \rho^{\frac{k-1}{M}}\Delta), \quad \forall k \in \mathbb{Z}_{\geq 1}, \tag{28}$$

then $\lim_{k\to\infty} \lambda_k = 0$.

Lemma 3.7 is proven in (Caruntu et al., 2011a) and is omitted here for brevity. By augmenting Problem 3.5 with constraint (28) the property $\lim_{k\to\infty} \lambda_k^* = 0$ is thus guaranteed, which is sufficient for asymptotic stability.

The developed robust MPC scheme for the constrained system (19) can be implemented by solving a single LP during each control cycle using an infinity-norm based candidate CLF as shown in (Caruntu and Lazar, 2011) and is omitted here.

4. EXPERIMENTAL RESULTS

This section presents the validation of the proposed networked one step ahead robust predictive control strategy based on the designed Luenberger observer. It was investigated using a real-time simulation test-bench based on the M220 Industrial plant emulator (M220, 1995), which can emulate an automated manual transmission (AMT) driveline with backlash nonlinearity and driveline flexibility. The one step ahead MPC scheme was implemented in Matlab/Simulink and real time experiments were conducted by using Real Time Windows Target, that allows external connection to the M220 Plant Emulator. The sampling period of the system was chosen as $T_s = 4$ms. Please note that on a real automotive drivetrain only angular velocities can be measured, so the full state will be estimated by the designed observer.

The upper bound of the delays that are induced by CAN was calculated using the methodology described in (Klehmet et al., 2008), resulting that $\tau^{max} = 2T_s = 0.008$s for each channel, which is used to apply the presented methodology to model the effects of the variable time delays as disturbances. Then, the bounds of the disturbances are explicitly taken into account by the robust one step ahead predictive control strategy described in Section 3. The delays are time-varying and uniformly distributed in the interval $[0, \tau^{max}]$.

The control objective is to reach a desired wheel angular velocity in a short time and to increase the passenger comfort by reducing the backlash effect. The axle wrap, which is calculated as the difference between the engine speed (divided by the total transmission ratio) and the wheel speed is used as a measure of the driveline oscillations.

The recursive feasibility of the robust one step ahead MPC scheme developed in this paper implies asymptotic stability. However, recursive feasibility is not a priori guaranteed and hinges mainly on the constraint (28) on the future evolution of λ_k^*. For all simulation scenarios case studies, the values $\Omega = 0.5$ and $M = 1$ proved to be large enough to guarantee recursive feasibility for the desired operating scenarios.

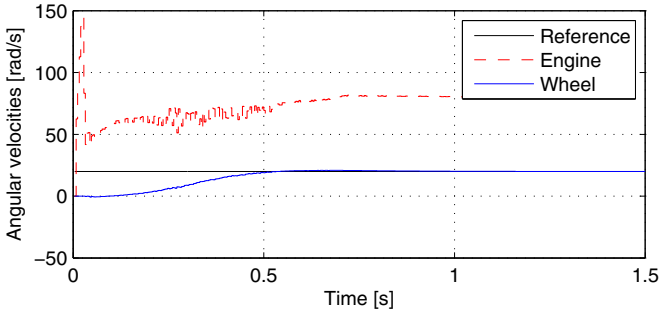

Fig. 5. Angular velocities.

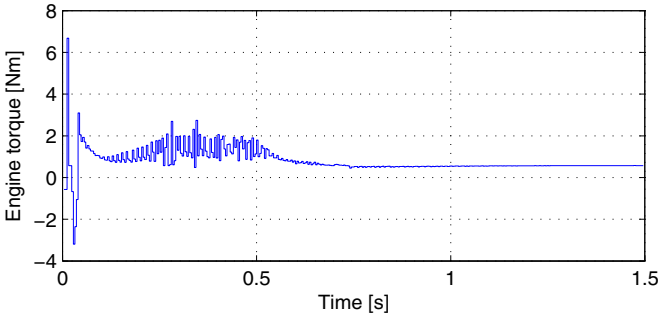

Fig. 6. Engine torque (control signal).

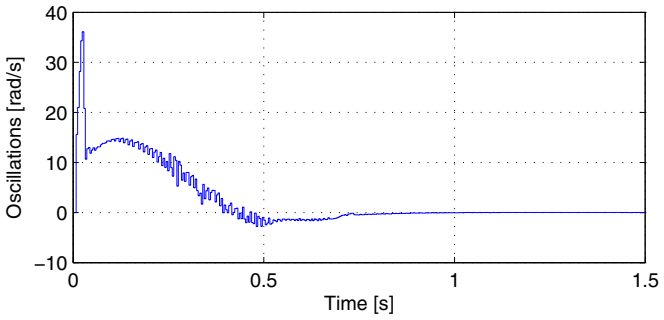

Fig. 7. Speed difference.

The engine and wheel angular velocities are illustrated in Fig. 5, where it can be seen that the system reaches the reference in a short time, having almost no overshoot when it approaches the reference wheel angular velocity. When the system is in the non-contact mode there is no torque transmitted to the driving wheels because of the backlash, so the wheel angular velocity is equal to 0. After the system enters the contact mode (6 sampling periods = 24 ms), the wheel angular velocity starts to increase. Also, the engine torque and the axle wrap are represented in Fig. 6 and Fig. 7.

The differences between the real states of the emulator and the estimated states are illustrated in Fig. 8 - Fig. 10 in which it can be seen that the estimated values of the states provided by the observer tend asymptotically to the real state.

5. CONCLUSIONS

This paper considered the design of a full state-feedback predictive controller based on a Luenberger observer with the

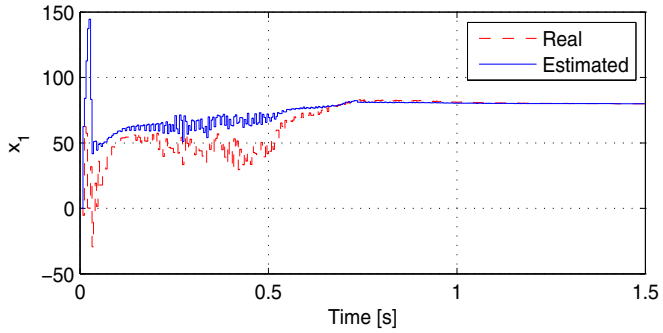

Fig. 8. Evolution of state x_1.

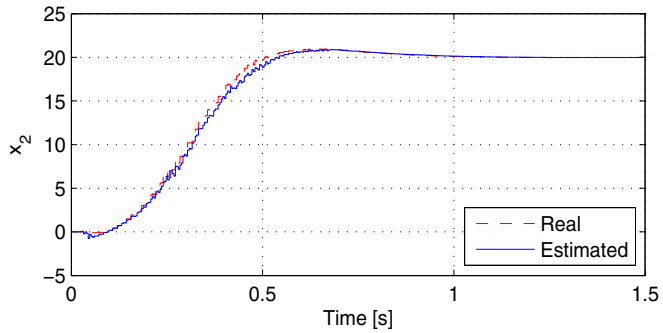

Fig. 9. Evolution of state x_2.

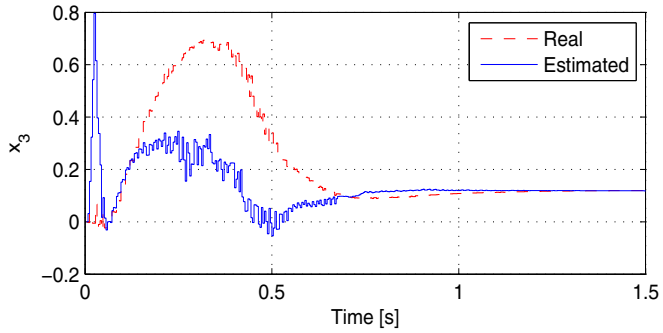

Fig. 10. Evolution of state x_3.

aim of compensating the backlash effects, while decreasing the influence of the network-induced time-varying delays on the closed-loop control performances over the CAN network. The designed robust one step ahead MPC strategy can handle the performance/physical constraints and explicitly takes into account the disturbances caused by the time-varying delays. Also, a flexible control Lyapunov function was employed to obtain a non-conservative ISS stability guarantee for the developed one step ahead MPC scheme. The proposed control strategy was tested on a real-time simulation test-bench including CAN communications and the results obtained illustrate that the proposed controller has good performances and it meets the required timing constraints.

REFERENCES

Ahmed-Ali, T., Karafyllis, I., and Lamnabhi-Lagarrique, F. (2013). Global exponential sampled-data observers for nonlinear systems with delayed measurements. *Systems & Control Letters*, 62, 539–549.

Alessandri, A. and Coletta, P. (2001). Design of Luenberger observers for a class of hybrid linear systems. In *Hybrid Systems: Computation and Control*, 7–18. Rome, Italy.

Caruntu, C.F., Balau, A.E., Lazar, M., van den Bosch, P.P.J., and Di Cairano, S. (2011a). A predictive control solution for driveline oscillations damping. In *Hybrid Systems: Computation and Control*, 181–190. Chicago, USA.

Caruntu, C.F. and Lazar, C. (2011). Robust MPC for TrueTime simulation of a vehicle drivetrain controlled through CAN. In *16th IEEE International Conference on Emerging Technologies and Factory Automation*. Toulouse, France.

Caruntu, C.F. and Lazar, C. (2012). Robustly stabilising model predictive control design for networked control systems with an application to direct current motors. *IET Control Theory and Applications*, 6, 943–952.

Caruntu, C.F., Lazar, M., Di Cairano, S., Gielen, R.H., and van den Bosch, P.P.J. (2011b). Horizon-1 predictive control of networked controlled vehicle drivetrains. In *18th IFAC World Congress*, 3824–3830. Milano, Italy.

Heemels, W.P.M.H., Lazar, M., van de Wouw, N., and Pavlov, A. (2008). Observer-based control of discrete-time piecewise affine systems: exploiting continuity twice. In *Conference on Decision and Control*, 4675–4680. Cancun, Mexico.

Jiang, Z.P. and Wang, Y. (2001). Input-to-state stability for discrete-time nonlinear systems. *Automatica*, 37, 857–869.

Juloski, A.L., Heemels, W.P.M.H., and Weiland, S. (2007). Observer design for a class of piecewise linear systems. *International Journal of Robust and Nonlinear Control*, 17, 1387–1404.

Klehmet, U., Herpel, T., Hielscher, K.S., and German, R. (2008). Delay bounds for CAN communication in automotive applications. In *14th GI/ITG Conference Measurement, Modelling and Evaluation of Computer and Communication Systems*. Dortmund, Germany.

Lazar, M. (2009). Flexible control Lyapunov functions. In *28th American Control Conference*, 102–107. St. Louis, MO, USA.

Lazar, M. and Heemels, W.P.M.H. (2008). Optimized input-to-state stabilization of discrete-time nonlinear systems with bounded inputs. In *27th American Control Conference*. Seattle, USA.

M220 (1995). *Industrial Emulator / Servo Trainer*. ecp Educational Control Products. [http://maelabs.ucsd.edu/mae171/controldocs/industrial.htm].

Natori, K., Oboe, R., and Ohnishi, K. (2008). Stability analysis and practical design procedure of time delayed control systems with communication disturbance observer. *IEEE Transactions on Industrial Informatics*, 4, 185–197.

Postoyan, R. and Nesic, D. (2012). A framework for the observer design for networked control system. *IEEE Transactions on Automatic Control*, 57, 1309–1314.

Rostalski, P., Besselmann, T., Maric, M., Van Belsen, F., and Morari, M. (2007). A hybrid approach to modelling, control and state estimation of mechanical systems with backlash. *International Journal of Control*, 80, 1729–1740.

Spinu, V., Dam, M., and Lazar, M. (2012). Observer design for DC/DC power converters with bilinear averaged model. In *Conference on Analysis and Design of Hybrid Systems*, 204–209. Eindhoven, The Netherlands.

Templin, P. (2008). Simultaneous estimation of driveline dynamics and backlash size for control design. In *IEEE International Conference on Control Applications*, 13–18. San Antonio, Texas, USA.